Small molecule-based approach for targeting CGG repeat expansion in Fragile X-associated Tremor/Ataxia Syndrome

M.Sc. Thesis

By

VEDANT DUSHANT SALVE

DISCIPLINE OF BIOSCIENCES AND BIOMEDICAL ENGINEERING

INDIAN INSTITUTE OF TECHNOLOGY INDORE

MAY 2022

Small molecule-based approach for targeting CGG repeat expansion in Fragile X-associated Tremor/Ataxia Syndrome

A THESIS

Submitted in partial fulfillment of the

requirements for the award of the degree

of

Master of Science

by

VEDANT DUSHANT SALVE

DISCIPLINE OF BIOSCIENCES AND BIOMEDICAL ENGINEERING

INDIAN INSTITUTE OF TECHNOLOGY INDORE

MAY 2022

INDIAN INSTITUTE OF TECHNOLOGY INDORE

CANDIDATE'S DECLARATION

I hereby certify that the work which is being presented in the thesis entitled **Small molecule-based approach for targeting CGG repeat expansion in Fragile X-associated Tremor/Ataxia Syndrome** in the partial fulfillment of the requirements for the award of the degree of **MASTER OF SCIENCE** and submitted in the **DISCIPLINE OF BIOSCIENCES AND BIOMEDICAL ENGINEERING, Indian Institute of Technology Indore**, is an authentic record of my own work carried out during the time period from August 2020 to May 2022 under the supervision of **Prof. Amit Kumar** HOD, BSBE, IIT Indore.

The matter presented in this thesis has not been submitted by me for the award of any other degree of this or any other institute.

Date: 30 May 2022
VEDANT DUSHANT SALVE

This is to certify that the above statement made by the candidate is correct to the best of my/our knowledge.

Signature of the Supervisor
Prof. Amit Kumar

VEDANT DUSHANT SALVE has successfully given his M.Sc. Oral Examination held on 5th May 2022.

Signature of Supervisor of MSc thesis
Prof. Amit Kumar

Convener, DPGC
05/05/2022
Prof. Prashant Kodgire

Date:

Signature of PSPC Member
Prof. Prashant Kodgire

Date: 05/05/2022

Date:

Signature of PSPC Member
Dr. Abhijeet Joshi

Date: 30th May 2022

Acknowledgment

Firstly, I would like to express my sincere and heartfelt gratitude to my research supervisor **Prof. Amit Kumar**, who always motivated me during my work. Without his guidance and support, this work would not be possible. I am thankful to **Dr. Prashant Kodgire** and **Dr. Abhijeet Joshi**, for being my PSPC members, their critical comments really helped me to improve my thesis work.

Here, I would like to thank my lab seniors, **Mr. Uma Shankar** and **Ms. Neha Jain** for their constant support and guidance in my work. I would like to express my gratitude to **Mr. Krishna Singh** for teaching me all the lab skills from the basics to the use of sophisticated instruments. Without his constant help, this work would not have been possible. I would also like to thank all of lab mates for their constant support and help. I would like to express my special thanks to my batchmates and my friends **Mr. Akshay Mehta** and **Mr. Piyush Goel** for their support and encouragement.

Last but not the least, I would also like to thank my family, especially my mother and father for always supporting me and believing in me, even in the most difficult of moments. Without their support and motivation, I would not have made it this far.

VEDANT DUSHANT SALVE

DEDICATED TO MY FAMILY AND FRIENDS

VEDANT DUSHANT SALVE

Abstract

Fragile X-associated tremor ataxia syndrome is a result of the expansion of 55 to 200 CGG nucleotide repeats in 5'UTR of Fragile X mental retardation 1. This expansion of CGG nucleotide repeats causes neuronal toxicity by two main pathogenic mechanisms. In the first case splicing alterations and formation of ribonuclear inclusions takes place as a result of the sequestration of specific RNA regulatory proteins by mRNA. While in the second pathogenic mechanism FMRPolyG which is a toxic homopolymeric protein is formed as a result of repeat-associated non-canonical translation (RANT). In this study, we have used a small molecule-based approach for targeting the CGG repeat expansion. FDA-approved drugs were screened against RNA library having a 1*1 internal nucleotide loop by fluorescence intercalator displacement assay. After performing screening of these molecules lead molecules were identified. These lead molecules were then checked for binding affinity with the target CGG repeat by fluorescence binding assay, Isothermal calorimetry titration, and electrophoretic mobility shift assay. Finally, to check the potency of these molecules in cell-based assay effect of drugs on protein aggregation and protein accumulation in the FXTAS cell model was studied. A significant decrease in protein aggregates was found in one of the lead molecules while the remaining lead molecules also showed a decrease in protein aggregation. These lead molecules showed positive results in cell-based assay further studies have to be done for these lead molecules.

Contents

List of Figures

List of Tables

Abbreviations

FXTAS	-	Fragile X-Associated Tremor/Ataxia Syndrome
FXS	-	Fragile X Syndrome
TNR	-	Trinucleotide Repeat
UTR	-	Untranslated Region
AONs	-	Antisense Oligonucleotides
FRDA	-	Friedreich ataxia
PSA	-	Polar Surface Area
FXPOI	-	Fragile X-Associated Primary Ovarian Insufficiency
FMR1	-	Fragile X Mental Retardation 1
IPTG	-	Isopropyl- β- D-1 Thiogalactopyranoside
TSA	-	Trichostatin A
POF	-	Premature Ovarian Failure
FSH	-	Follicle Stimulating Hormone
RANT	-	Repeat-Associated Non-ATG Translation
NCD	-	Naphtyridine Carbamate Dimer
PLA2	-	Phospholiase A2
FID	-	Fluorescence Intercalator Displacement Assay
FBA	-	Fluorescence Binding Assay
ITC	-	Isothermal Titration Calorimetry
SDS PAGE	-	Sodium Dodecyl Sulphate Polyacrylamide Gel Electrophoresis
APS	-	Ammonium Persulphate
TEMED	-	Tetramethylethylenediamine
MQ	-	Milli Q

TO	-	Thiazole Orange
DNA	-	Deoxyribose Nucleic Acid
RNA	-	Ribose Nucleic Acid
EMSA	-	Electrophoretic Mobility Shift Assay
HEK cells	-	Human Embryonic Kidney cells

Chapter 1 : Introduction

Fragile X-associated tremor/ataxia syndrome (FXTAS) and fragile X syndrome (FXS) are neurological disorders associated with unstable expanded repeats i.e., trinucleotide repeats[1,2]. Trinucleotide repeats are considered a group of a special class of microsatellites and when these microsatellites increase beyond their threshold numbers may lead to diseases. There are many neurological disorders caused by different trinucleotide repeats and the statistics of such disorders are increasing day by day[3]. Trinucleotide repeat (TNR) diseases can be classified into two classes depending on the location of the repeats. In FRAXA non-coding repeats is found in 5′ untranslated region (UTR), whereas in Friedrich ataxia it is found in introns and in myotonic dystrophy 1 it is found in 3′UTRs. Although TNR diseases can differ in their repeat sequences (CCG, GAA, CGG, CAG, CTG) along with their disease-causing mechanism they have similarities too i.e., the extremeness of these trinucleotide repeat disease depends on the number of repeats.

Different therapeutic strategies to target TNR diseases include (i) RNA interference (RNAi) or antisense oligonucleotides (AONs) , (ii) antisense oligomers , and (iii) modified antisense oligomers, siRNAs or miRNAs[4]. Nowadays, small molecule-based therapies are preferred. There are over 40 caused as result of expansion of repeated sequences which also includes Friedreich ataxia (FRDA) and Fragile X syndrome (FXS). Molecular pathology of these diseases is not well understood. It is proposed that repressive chromatin formation and unusual structures of DNA play a role in the pathology. Hybrids of RNA/DNA (R loops) are formed in cells of patients on the expanded repeats of endogenous FXN and FMR1 genes which are associated with Friedreich ataxia and Fragile X syndrome. R loops are transcription-dependant. Due to co-localisation of these loops with H3K9me2 chromatin mark this results in difficulty in transcription for RNA polymerase II. These R-loops can also cause transcriptional silencing of FXN. This is caused due to their increased levels by camptothecin which is a DNA topoisomerase inhibitor. This is direct evidence that these R-loops are involved in the pathology of trinucleotide repeat disorders as these R-loops acts as trigger for promoting FXN and FMR1 silencing[5]. Hence these R-loops

can be a target for potential new therapeutic approach for the treatment of disorders.

Fragile X syndrome (FRAXA), FXTAS, and fragile X-associated primary ovarian insufficiency (FXPOI) are neurological diseases caused by expanded CGG repeats. In the 5′ UTRs of fragile X mental retardation 1 (FMR1) gene CGG repeats increases leading to the diseases which are mentioned above. The gene can function as normal (5–55), premutation (55–200), and full mutation (> 200) depending on the number of repeats.[6]

1.1 Fragile X-Syndrome (FXS)

The occurence of FXS is inconsistent worldwide, causing 1 in 7000 females and 1 in 4000 males[7]. Leading cause of intellectual disability is Fragile X-Syndrome after Downs's syndrome[8]. When an affected person showed intellectual disability, macro-orchidism and dysmorphic features FXS was first reorted[9]. Fragile X syndrome is so named as it shows fragility at the terminal end of the long arm of the X chromosome and it was identified by Dr. Lubs as a cytogenetic marker[10]. Earlier karyotyping was used for diagnosis of FXS in patients with risk of FXS but now a days polymerase chain reaction based tests are which provide more sensite and specific data[8]. FXS can be treated by activating the FMR1 gene or by treatment of the symptoms aroused due to the disease. In vitro studies revealed that 5- azadC which is an inhibitor of methyltransferase, along with 4-phenylbutyrate, butyrate and trichostatin A (TSA) which are histone deacetylase inhibitors can successfully restore the of FMR1 gene activity. Because of increased cellular apoptotic activity the same combination of drugs didn't work in in-vivo conditions. For the treatment of FXS symptoms folic acid[11], valproic acid[12], Lacetylcarnitine[12], clonidine, melatonin[13], methylphenidate, and amphetamine salts are used but some side effects can also be observed[14]. Along with pharmacologic treatment cognitive and behavioral therapies can also benefit patients suffering from fragile X-syndrome[15–17].

1.2 Fragile X-associated tremor/ataxia syndrome (FXTAS)

It is a neurodegenerative disease which mostly affects males[18]. Fragile X-associated tremor/ataxia syndrome is a hereditary disorder thus its diagnosis

is crucial to determine the risk of developing disease in the family. It is caused due to the increase in the numbers of expanded CGG repeats in 5′ UTR of the FMR1 gene and the numbers lies in the pre mutation range. The protein that is fragile X mental retardation protein (FMRP) is produced in normal concentration but in the brain cells and leukocytes the level of mRNA is increase[19,20] which can later leads to cellular injury, causing morbidity and ataxia in aging men[21,22]. The carriers of premutation of FXTAS is 1 among 260 females[23] and 1 among 813 males[24]. The penetrance of FXTAS differs in both the sexes i.e., male and female and it highly depends on the age such as 40% of male carriers are over 50 years of age[25] while 8% of female carriers are over 40 years of age. As it is recently reported so most physicians are not familiar with the symptoms concerned with it; therefore, the incidents of incorrect diagnosis may increase. Hagerman et al. have given guidelines and criteria for the diagnosis of the FXTAS and it can reduce the probability of erroneous diagnosis[26]. Various therapeutic agents are available which treat the symptoms which are associated with fragile X-associated tremor ataxia syndrome like amantadine, varenicline, benzodiazepines, gabapentin. levetiracetam, clonazepam, clozapine, nadololand some acetylcholinesterase inhibitors. More studies are required to come up with better strategies against the disease[27,28,28].

1.3 Fragile X-associated primary ovarian insufficiency

Increase in the number of CGG repeats in Fragile X mental retardation gene 1 causes Fragile X-associated primary ovarian insufficiency i.e., in 5′UTR. CGG repeats of about 55–200 copies in females increases the chances of developing hypergonadotropic hypogonadism. The outcome of this disease leads to end of menstruation before reaching the age of 40 years and the condition is often mention as premature ovarian failure (POF) in medical terms. Warren et al. had reported the frequency of occurrence for these disease being 1 among 350 females. Primary ovarian insufficiency leads to increase level of follicle-stimulating hormone (FSH) and decreased level of anti-Mullerian hormone in the body leading to abnormal endothelial functions[29], bone fracture[30], and early onset of coronary heart diseases[31]. Early menopause in woman can arise several physiological problems which can include anxiety,

depression, somatization sensitivity, and other related problems[31]. Treatment for these symptoms are available but no treatment is yet reported to alter the infertility caused by this disease.

1.4 Small molecules mediated therapeutic approach for CGG repeat disorders

Small molecules can identify secondary and tertiary structures of nucleic acids i.e., DNA or RNA which includes junctions, loops, and bulges and it does not depends on their complementary sequences. Aminoglycosides are source from where small molecules which can identify RNA are derived. Small molecules have low molecular weight (~ 500), low polar surface area (PSA), and mostly by electrostatic interactions the remain bound to RNA. Small molecules are planar compounds due to this they provide enough space for interactions between RNA and small molecule. These interactions include hydrogen bonding, hydrophobic interactions with the benzene ring of the base pairs and π-π interactions[5]. Due to all of these interactions the binding affinity of these small molecules with RNAs increases and it does not depends on the sequence complementarity. Targeting RNA by small molecules and using it as therapeutics is very difficult due to the dynamic structure, anionic nature and flexibility of RNA.

Increase in numbers of CGG repeats leads to different neurodegenerative diseases causing arrival of different symptoms, targeting these expanded CGG repeats by various small molecules may provide a different prospect to treat these diseases. Expansion of these repeats causes disease initiation and progression by sequestering proteins important for the inhibition of the disease or by RAN translation (repeat-associated non-ATG translation). Small molecules bind to these CGG repeats to reduce the pathogenicity of the disease. It was reported in study that akyl and phenolic side chains are crucial for recognition of CGG repeats[32]. It is also reported that small molceules have the ability to inhibit the toxicity which is result of these repeats. Many small molecules can also target these CGG repeats such as naphthyridine carbamate dimer (NCD), phospholipase A2 (PLA2) inhibitors[33], 2′-O-methyl phosphorothioate compound 1a[34]. Zhu and his group have synthesized carboxyl-functionalized Fe_3O_4 magnetic nanoparticles based nanoprobe for detection of CGG repeats, which can be of great help in detection of these

CGG repeat-associated diseases[35]. Piperine has been reported to improve the splicing defects and translation in FXTAS cell model system[36]. There are various reports which suggest small molecules can target these CGG repeats. In this study, we have screened the FDA-approved small molecules for their binding affinity with specifically with CGG repeat by performing fluorescence intercalator displacement assay (FID). RNA library having 1*1 internal nucleotide loop was constructed and along with G-G mismatch all other possible mismatches along with the control that is RNA having A-U canonical base pairing were used. This RNA having canonical base airing served as control RNA.

Given below is the RNA library having various 1*1 internal nucleotide loop.

No.	RNA
1	5’C**A**G/3’C**G**G
2	5’C**C**G/3’C**A**G
3	5’C**G**G/3’C**A**G
4	5’C**C**G/3’C**U**G
5	5’C**A**G/3’C**C**G
6	5’C**U**G/3’C**C**G
7	5’C**G**G/3’C**G**G
8	5’C**A**G/3’C**A**G
9	5’C**C**G/3’C**C**G
10	5’C**U**G/3’C**U**G
11	5’C**A**G/3’C**U**G

Table 1 RNA library having 1*1 internal nucleotide loops

After performing the FID assay we found lead molecules which showed positive displacement specifically to CGG. These lead molecules were then further studied for their binding potential by various assays like fluorescence binding assay (FBA), isothermal calorimetry titration (ITC) assay.

1.5 Objective

Synthesis of RNA library

Screening of FDA-approved small molecules by Fluorescence Intercalator Displacement Assay

To perform binding studies of lead molecules by

- Fluorescence Binding Assay
- Isothermal Calorimetry Titration Assay

To perform cell-based assay of lead molecules

Chapter 2 : Material and Methodology

2.1 Expression and Purification of T7 polymerase

For the in-vitro transcription of RNA, an RNA polymerase enzyme is required which will synthesize RNA from the template DNA. For this purpose T7 RNA polymerase was chosen. For the in-vitro transcription of RNA, bacterial RNA polymerase like T7 RNA polymerase is very effective. They consist of only one polypeptide chain and thus dissociation initiation factor is not required.[37] The T7 polymerase has a single subunit of 100 kDa, it is very specific to its promotor which is 23 base pairs long. Due to this specific reason, it is very suitable for producing transcripts of range 30 nucleotides to 10^4 nucleotides.

Overexpression of this T7 polymerase was done by using Isopropyl β-D-1-thiogalactopyranoside (IPTG). It is the molecular mimic of allolactose which is a promoter of the *lac operon* system (Lactose operon) IPTG binds with the lac repressor protein and dissociates the tetrameric lac repressor from the lac operator region through an allosteric action, thereby allowing the transcription of genes on the lac operon. Unlike the normal process of allolactose induction, the IPTG induction lasts for a longer period. Although IPTG mimics the structure of allolactose, unlike allolactose, it consists of a sulphur bond that stabilizes the bonding by creating a bond that is nonhydrolyzable by cellular enzymes, it prevents the cell from hydrolyzing the inducer. The concentration of IPTG inside the cell thus remains constant, and gene expression is not inhibited during the experiment.

Preparation of Primary culture

1. Luria Bertani broth 25 ml
2. Antibiotic - Ampicillin 12.5 µl (100 mg/ml)
3. Antibiotic - Chloramphenicol 12.5 µl (68 mg/ml)
4. A single colony from agar plates

Once all of the above was added the primary culture was kept in an incubator shaker at 37 ^{o}C, 220 RPM overnight.

Preparation of Secondary culture

1. Luria Bertani broth 100 ml

2. Antibiotic - Ampicillin 50 µl (100 mg/ml)
3. Antibiotic - Chloramphenicol 50 µl (68 mg/ml)
4. 0.6 ml of primary culture

After inoculation with 0.6 ml primary culture, the culture was incubated in an incubator shaker at 37 ^{o}C, 220 RPM till the optical density reached 0.4 to 0.6. This particular OD signifies that the cells are in the log phase. After which induction was done by Isopropyl- β- D-1 thiogalactopyranoside (IPTG).

Lysis of cells

After 4 hrs of incubation, media having bacterial cells was transferred into 50 ml centrifuge tubes and was centrifuged at 5000 RPM for 15 minutes at 4 ^{o}C. After which the pellet was obtained, the supernatant was discarded. For checking whether induction by IPTG was successful or not, 2ml of samples were collected in microcentrifuge tubes of primary, before induction, and after induction samples. These samples were also centrifuged and pellet was obtained after discarding the supernatant.

The pellet was then dissolved in lysis buffer (composition of which is given below). After resuspending the pellet in the lysis buffer sonication was done.

Composition of lysis buffer

Sr. No.	Components	Concentration	Role
1	NaCl	300 mM	Regulate osmolarity
2	Glycerol	5%	Reduce hydrophilic interactions
3	Tris (PH 8)	25 mM	Regulate pH

Table 2 Composition of lysis buffer

Ionic salts like NaCl regulates the osmolarity of the lysate, Buffering salts like Tris-Cl regulates the pH of the solution, glycerol in the buffer helps to reduce the hydrophilic interactions, and it helps in solubilizing the protein.

For sonication, a probe sonicator was used. It was operated at an amplitude of 65 and in cycles of 1 sec up and 2 sec down. After sonication, the lysate was centrifuged for 1 hr 20 minutes at 9500 RPM and 4 ^{o}C. After which a pellet and supernatant were obtained. The supernatant was collected and the pellet

was discarded. The supernatant obtained from this was then used as sample for checking whether induction by IPTG was successful or not.

SDS PAGE to check the expression of T7 polymerase

SDS PAGE was performed to check the expression of the target protein i.e. T7 polymerase. Given below is preparation of the reagents required for SDS PAGE.

Compositions of reagents

Coomassie brilliant blue staining solution

Reagent	Final concentration
Coomassie brilliant blue R-250	0.05 %
Methanol	50%
Glacial acetic acid	10%
Water	To make up volume

Table 3 Composition of Coomassie brilliant blue staining solution

Coomassie brilliant blue R-250 is a dye used for staining the gels after the gel run; it will bind with protein bands present in the gel. This dye gives a visible confirmation of bands present over the gel. It is dissolved in solvents like methanol and acetic acid.

De-staining solution

Reagent	Final Concentration
Methanol	30%
Glacial acetic acid	10%
Water	To make up volume

Table 4 Composition of De-staining solution

The de-staining solution is used for removing the dye from the gel other than the protein band regions.

Tris-glycine electrophoresis buffer

Reagent	Final Concentration
Tris base	250 mM
Glycine	1.9 M
SDS	1%
Water	To make up volume

Table 5 Composition of Tris-glycine electrophoresis buffer

Tris base provides the buffering function while glycine acts as the weak acid, which could be present in two forms, either the Zwitterionic form (neutral) or the Glycinate ion (negative). Upon providing the power to electrophoresis unit, the Glycinate ion due to being negatively charged migrates away from the negative electrode (cathode) it moves towards the sample at the stacking region where PH is so low that they lose their charge and slow down. As this flow of ions reaches the resolving region, it creates a stable electric field which provides an ideal environment for protein migration. Sodium Dodecyl Sulphate is a strong detergent, and it linearizes the protein.

Resolving Gel

Reagent	Resolving Gel (10%)
Water	4.1 ml
Acrylamide (30%)	3.3 ml
Tris (1.5 M pH 8.8)	2.6 ml
SDS (10 %)	100 µl
APS (10 %)	100 µl
TEMED	10 µl
Total Volume	10 ml

Table 6 Composition of Resolving Gel

30% Acrylamide solution is prepared by adding acrylamide and bis acrylamide in the ratio of 29:1, respectively. During the polymerization reaction, a crosslink is formed between bis-acrylamide and acrylamide, which is induced by Ammonium Per Sulphate (APS) which decomposes down to form free radicals, these free radicals induce the polymerization. tetramethylethylenediamine (TEMED) is a compound that stabilizes free

radicals and allows them to exist for a longer time; this increases the rate of polymerization of the gel. When the power is turned on then initially negatively charged Cl- ions start migrating then followed by negatively charged glycinate ions, the proteins are sandwiched between these two ionic fronts, the PH of resolving gel is 8.8 which increases the migration rate of glycinate ions which leaves the proteins behind and the resolution of proteins begins in the denser resolving medium.

Stacking Gel

Reagent	Stacking Gel (5 %)
Water	2.73 ml
Acrylamide (30%)	0.67 ml
Tris (1.5 M pH 6.8)	0.5 ml
SDS (10 %)	40 µl
APS (10 %)	40 µl
TEMED	4 µl
Total Volume	4 ml

Table 7 Composition of Stacking Gel

Preparation of Sample

3 µl BSA, 27 µl water, and 5 µl dye were mixed to prepare the BSA, and 30 µl of each sample (Primary, -IPTG, and +IPTG) were mixed with the 5 µl of dye. These prepared samples were heated at 92^0C for 10 minutes in a dry bath. After the 10 minutes of dry heating, samples were allowed to cool at room temperature, and then samples were loaded on SDS-PAGE gel for electrophoresis along with BSA.

Purification of T7 polymerase

Once induction was confirmed by observing the SDS gel the pellet obtained initially was resuspended in 20-25 ml of lysis buffer. This was followed by sonication of the lysate. After sonication, the lysate was then centrifuged for 1 hr 20 minutes at 4ºC and 7500 rpm. After centrifugation, the supernatant was collected and the pellet was discarded. This supernatant was then used for the purification of T7 polymerase.

Given below are the compositions of buffers used for the protein purification.

Low Salt washing buffer

Reagent	Final concentration
NaCl	300 mM
Tris (pH 8.0)	25 mM
Imidazole	20 mM

Table 8 Composition of Low Salt washing buffer

High Salt washing buffer

Reagent	Final concentration
NaCl	1 M
Tris (pH 8.0)	25 mM
Imidazole	20 mM

Table 9 Composition of High Salt washing buffer

Elution buffer

Reagent	Final concentration
NaCl	300 mM
Tris (pH 7.0)	50 mM
Imidazole	300 mM
Glycerol	5 %

Table 10 Composition of Elution buffer

The purification of T7 polymerase was done by both manual method and by sung AKTA pure. In AKTA pure His Trap FF 5ml was used for the purification. His trap FF 5 ml Column is a prepacked column of Nickel Sepharose fast flow which contains agarose beads of 90 µm infused with an immobilized chelating group. His trip is made up of biocompatible polypropylene, the whole system is charged with Ni^{2+} ions which have an affinity with histidine-tagged proteins. SDS PAGE was also done for the purified protein.

2.2 PCR amplification of template

For the in-vitro transcription of the RNA, a DNA template is required. This was obtained by performing PCR. The sequences for DNA templates used for RNA preparation are as below.

Sr. No.	Oligo Name	Sequence 5' to 3'
1	5'C**A**G/3'G **G**C	GGGAGAGGGTTTAAT**CAG**TACGAAAGTA**CGG**ATTGGATC CGCAAGG
2	5'C**C**G/3'G **A**C	GGGAGAGGGTTTAAT**CCG**TACGAAAGTA**CAG**ATTGGATC CGCAAGG
3	5'C**G**G/3'G **A**C	GGGAGAGGGTTTAAT**CGG**TACGAAAGTA**CAG**ATTGGATC CGCAAGG
4	5'C**C**G/3'G **U**C	GGGAGAGGGTTTAAT**CCG**TACGAAAGTA**CTG**ATTGGATC CGCAAGG
5	5'C**A**G/3'G **C**C	GGGAGAGGGTTTAAT**CAG**TACGAAAGTA**CCG**ATTGGATC CGCAAGG
6	5'C**U**G/3'G **C**C	GGGAGAGGGTTTAAT**CTG**TACGAAAGTA**CCG**ATTGGATC CGCAAGG
7	5'C**G**G/3'G **G**C	GGGAGAGGGTTTAAT**CGG**TACGAAAGTA**CGG**ATTGGATC CGCAAGG
8	5'C**A**G/3'G **A**C	GGGAGAGGGTTTAAT**CAG**TACGAAAGTA**CAG**ATTGGATC CGCAAGG
9	5'C**C**G/3'G **C**C	GGGAGAGGGTTTAAT**CCG**TACGAAAGTA**CCG**ATTGGATC CGCAAGG
10	5'C**U**G/3'G **U**C	GGGAGAGGGTTTAAT**CTG**TACGAAAGTA**CTG**ATTGGATC CGCAAGG
11	5'C**A**G/3'G **U**C	GGGAGAGGGTTTAAT**CAG**TACGAAAGTA**CTG**ATTGGATC CGCAAGG
12	Forward Primer	GGCCGGATCCTAATACGACTCACTATAGGGAGAGGGTTT AAT
13	Reverse Primer	CCTTGCGGATCCAA

Table 11 Sequences of DNA templates used for RNA preparation

For amplification of the template by PCR following concentrations of reagents were used.

Reagent	Working Concentrations
Buffer (without $MgCl_2$)	1 X
$MgCl_2$	4.25 mM
dNTPs	0.33 mM
Forward primer	2 µM
Reverse primer	2 µM
Template	6 µM
DMSO	10% V/V
Taq Polymerase	0.5 µl for 25 µl

Table 12 PCR reaction composition

2.3 In-vitro synthesis of RNA

To confirm the activity of the protein in-vitro reaction of 25 µl was done initially and once the activity was confirmed 500 µl invitro reaction was done.

In-vitro reaction

Reagent	Volume	Volume
Transcription buffer (10 X)	2.5 µl	50 µl
rNTPs (200 mM)	1 µl	20 µl
Template	12 µl	240 µl
T7 polymerase	9.5 µl	190 µl
Total volume	25 µl	500 µl

Table 13 Composition of in-vitro reaction

The product of the in-vitro reaction was then loaded onto the UREA PAGE gel. After the gel was run under UV bands of RNA were observed. These bands were then cut and RNA was then eluted from the gel by dipping the gel in 300 mM NaCl overnight at 4 ^{o}C.

The next day butanol wash was done twice. After which the upper layer was discarded. Then the supernatant was stored in chilled ethanol at – 80 ^{o}C.

Centrifugation was done at 4 ^{o}C, 14,000 RPM for 20 minutes and again it was stored in chilled ethanol after discarding the upper layer.

The next day, evaporation of ethanol was done in rotavapor till the ethanol was completely evaporated. After this, the RNA was dissolved in 50 µl of autoclaved MQ water. This was followed by the desalting of RNA in the PD10 desalting column. After desalting RNA was lyophilized to acquire high purity RNA. Once lyophilization was done the RNA is then dissolved in MQ water and its readings were taken with help of nanodrop to acquire concentration and A260/280 ratio.

2.4 Fluorescence Intercalator Displacement (FID) Assay

For the identification of nucleic acid binding ligands, the FID assay is a convenient tool. For the FID assay Thiazole orange (TO) was used as an indicator. The assay was performed with RNA library against 33 FDA-approved small molecules. When thiazole orange binds to the RNA fluorescence is observed which is detected with help of a microplate reader. An excitation wavelength of 480nm and an emission wavelength of 530nm was used.

For control, well readings of fluorescence of buffer, buffer plus thiazole orange, thiazole orange plus RNA were taken. All of the readings were taken in duplicates to minimize the error. The experiment was performed on a 96 well corning half-area black plate, potassium phosphate having 50 mM KCl was used as a buffer. Every well had the following contents – total volume 50 µl, 1X buffer, 500nm RNA and 1µM thiazole orange. The wells were filled with this composition and fluorescence readings were taken. After readings were taken, different small molecules were added to the wells. This was followed by an incubation period of 10 minutes. After the incubation period readings were taken to observe the change in fluorescence.

For plotting the graph, the control i.e. RNA plus thiazole orange was considered as 100 percent and with respect to this fluorescence of other samples was converted into percentage. Those small molecules which will displace thiazole orange and bind to the RNA will result in decrease in fluorescence, and these will be our lead molecules. 5'CAG/3'CUG RNA is control, those molecules which will decrease fluorescence with this RNA will not be considered for further binding studies.

2.5 Fluorescence Binding Assay

Movement of electron from higher energy state to lower energy state when it has moved to higher energy state by absorbing electromagnetic radiation of high energy results in emission phenomenon of visible light which is called as fluorescence.[38] The energy released during emission depends on the chemical environment of the electron. And the time frame for electron to get excited and to again go to lower energy state is around 10^8 seconds.[38] In this study we have observed change in fluorescence intensity of FDA approved small molecules after binding with RNA. The fluorescence binding assay was performed on Corning half area black 96 well plate at room temperature. The excitation and emission wavelengths of these molecules were already known. While preparing ligand and sample it was made sure that in each well the concentration of small molecule will be same. The experiment was done in duplicates. Initially in all wells ligand was poured in all of the wells. After this the RNA sample was serially diluted till the 11^{th} well. Last well did not have any RNA and was kept as control. After performing the assay readings were taken in Synergy H1 multi-mode microplate reader. The assay was performed with lead molecules obtained after screening by FID.

Analysis of the data was done with the help of Sigma Plot 12.0 software, in which data fitting was done by the following binding equation :

$df = B_{max}*abs(x)/K_{D1}*abs(x) + B_{max}1*abs(x)/k_{D2}*abs(x)$

where,

B_{max} = maximum number of binding sites

K_D = equilibrium dissociation constant

2.6 Isothermal titration calorimetry (ITC) assay

For illustration of complete thermodynamic profile of binding interactions between two molecules isothermal titration calorimetry is the most robust technique.[39–41] For studying interactions between varieties of biological molecules ITC plays promising role.[41] For study of binding interactions between small molecules and biological target ITC can be used. It can help to determine relative affinity between the target biological compound or molecule and small molecules. In ITC assay heat absorbed or released during interaction between two molecules is directly measured by calorimeter.[42] With the help of ITC various thermodynamic parameters like enthalpy, entropy, association constant can be determined by following formula.

$\Delta G = -RT \ln Ka = \Delta H - T\Delta S$

where,

R = Gas constant

T = Temperature

ΔH = Enthalpy

ΔS = Entropy

Ka = Association constant

Two cells are present in the micro calorimeter one is reference cell while the other is sample cell. Temperature difference between these two cells is monitored by a heat sensing device. Initially the difference in temperature between these two cells is zero. But when small volume of sample is added into the sample cell as a result of interaction between reactant and sample change in temperature takes place which is monitored. After this both cells are again returned to the same temperature. After this, small volumes of sample is added into the sample cell and after each addition change is monitored. This continues till the equilibrium is reached where the interactions become zero and thus difference in temperature between the two cells remains zero. Various thermodynamic binding parameters are determined by plotting. For this study in reference cell water was kept. While in sample cell our sample that is RNA and ligand (small molecules) were kept. RNA and small

molecules were dissolved in KPO_4 buffer. MicroCal Origin Software was used for plotting the final binding isotherm.

2.7 Cell Based Assay

After the binding studies we have also checked whether these lead molecules are able to inhibit the non-canonical RAN translation. Hallmark of FXTAS is intranuclear inclusions which are result of FMRPolyG protein. This FMRPolyG protein is rich in glycine. For this study HEK cells were chosen. They were transfected with plasmid having CGG*99 repeats incorporated in human 5'UTR of FMR1 sequence. This results in expression of FMRPolyG protein. When small molecule binds to the hairpin of RNA this will cause inhibition of the RAN translation which will result in reduction of protein mediated toxicity. The cells were treated with lead molecules and the effect on protein aggregation was observed.

Chapter 3 : Results

3.1 Expression of T7 polymerase by IPTG induction

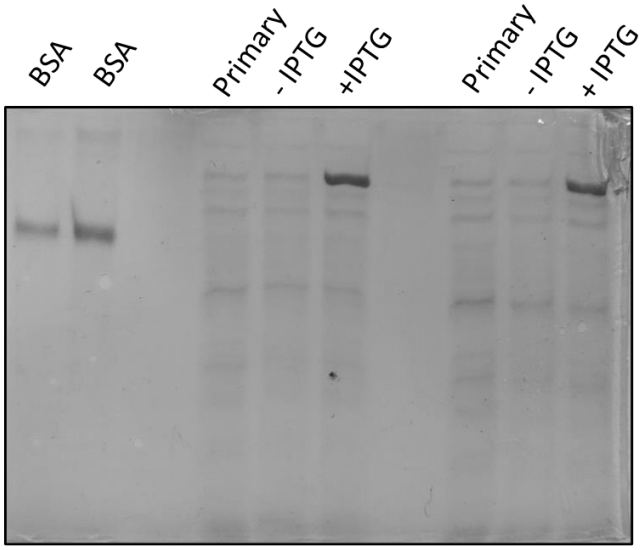

Figure 1 SDS PAGE Gel Image - Result of IPTG induction

After induction with help of IPTG, SDS PAGE gel was run to confirm the induction and expression of our protein of interest i.e. T7 polymerase. As we can see in figure 1, intense band was observed in after induction samples compared to primary and before induction sample which suggests induction was successful.

3.1.1 Purification of T7 polymerase by manual method

OD – Nanodrop

	Concentration (mg/ml)
Flow-through	7.828
High Salt	0.164
Low Salt	0.001
50 mM Imidazole	0.020
100 mM Imidazole	0.409
300 mM Imidazole 1	**1.723**
300 mM Imidazole 2	**5.014**
300 mM Imidazole 3	**3.588**

Table 14 Concentration of protein obtained by purification

Blank - 300 mM Imidazole

Protein was purified from manual method with highest OD 5.014 mg/ml.

SDS PAGE gel was also run to confirm the purity of the target protein.

SDS PAGE result of purified protein by manual method

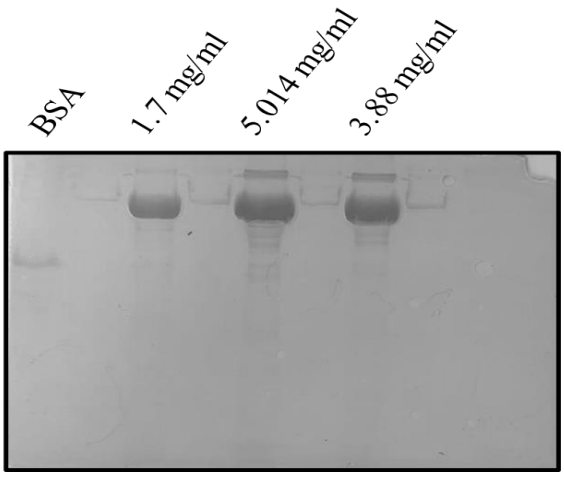

Figure 2 SDS PAGE - Result of protein purification by manual method

Figure 2 shows SDS PAGE result of the purified protein. Proteins with different concentrations obtained after purification along with BSA were run on the gel. The target protein has higher molecular weight than BSA thus its bands were observed above the band of BSA.

3.1.2 Purification of T7 by AKTA pure

Concentrations of protein obtained after elution are given below.

Sr. No.	Concentration (mg/ml)	Sr. No.	Concentration (mg/ml)
1	0.581	9	0.377
2	0.949	10	**1.336**
3	**1.977**	**11**	0.452
4	0.165	12	0.218
5	**1.457**	**13**	**2.264**
6	0.816	14	0.444
7	0.501	15	0.554
8	0.229	16	0.224

Table 15 Concentration of protein obtained by purification

SDS PAGE result of purified protein by AKTA

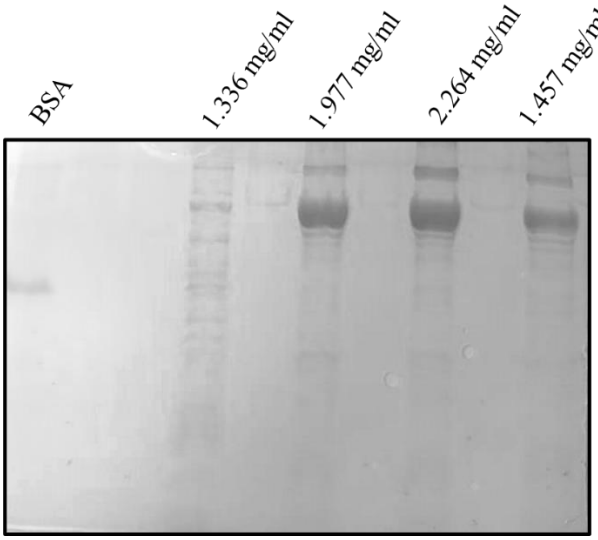

Figure 3 SDS PAGE Result of Protein purification by AKTA pure

Figure 3 shows SDS PAGE result of target protein purified by AKTA pure. Similarly, as in case of figure 2, target protein bands were observed comparably at higher position as compared to BSA.

3.2 Invitro transcription of RNA library

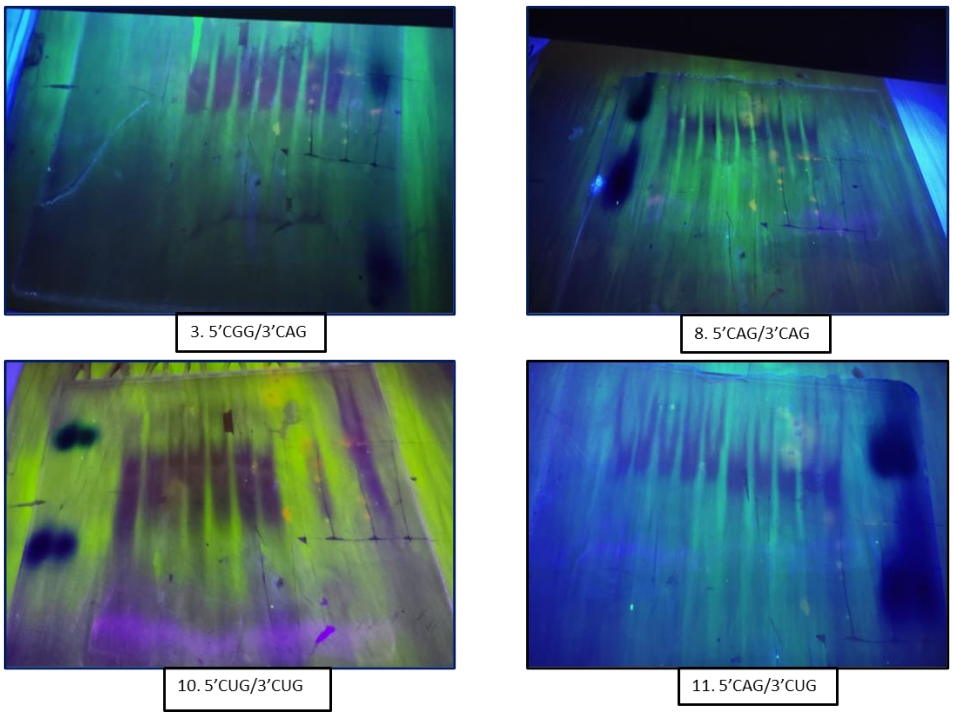

Figure 4 Result of in-vitro transcription of RNA. Gel image under UV light

Figure 4 shows some of the results of in-vitro transcription of RNA. Similarly, for all of the 11 RNA in RNA library in-vitro reaction was performed. After observing the band of RNA under UV light on the gel, it was cut and after the purification process, pure RNA was obtained. After purification process concentration of RNA was determined with the help of nanodrop.

3.3 Fluorescence Intercalator Displacement Assay

3.3.1 FID – RNA 5’CAG/3’CGG – TO against 33 compounds

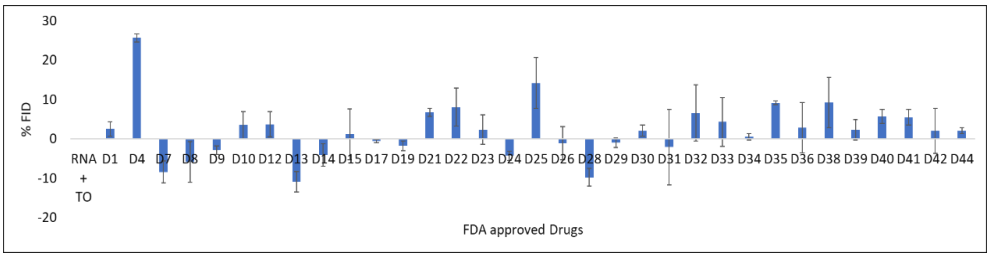

Figure 5 Percentage FID data of 5'CAG/3'CGG

After performing FID assay for 5’CAG/3’CGG we found D4 showed maximum displacement, apart from D4, D25, D35 and D38 also showed good positive displacement value.

3.3.2 FID – RNA 5’CCG/3’CAG – TO against 33 compounds

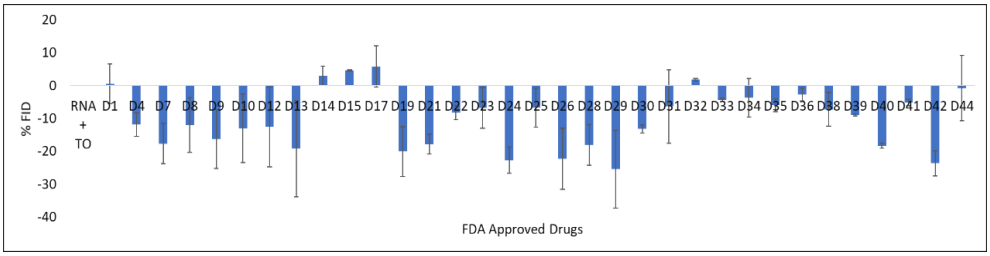

Figure 6 Percentage FID data of 5'CCG/3'CAG

As we can see from the graph drugs – D14, D15, D17 and D32 showed positive displacement of thiazole orange for 5’CCG/3’CAG which has a C-A mismatch. While remaining drugs increased the overall fluorescence percentage thus they did not displace thiazole orange.

3.3.3 FID – RNA 5’CGG/3’CAG – TO against 33 compounds

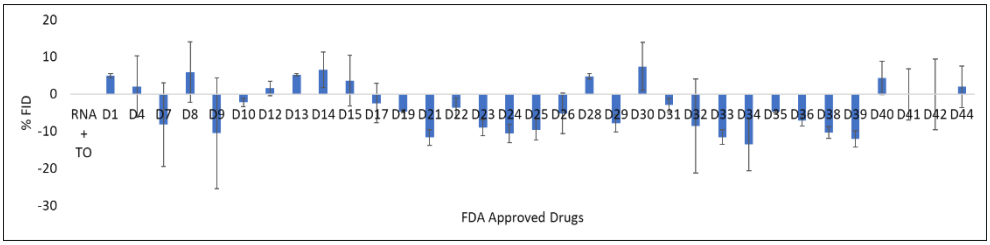

Figure 7 Percentage FID data of 5'CGG/3'CAG

For 5’CGG/3’CAG RNA which has G-A mismatch drugs D1, D4, D8, D12, D13, D14, D15, D28, D30, D40 and D44 showed a decrease in the fluorescence value out of these, D30 showed maximum reduction in the fluorescence value. In the case of other drugs, no such decrease in fluorescence was observed.

3.3.4 FID – RNA 5’CCG/3’CUG – TO against 33 compounds

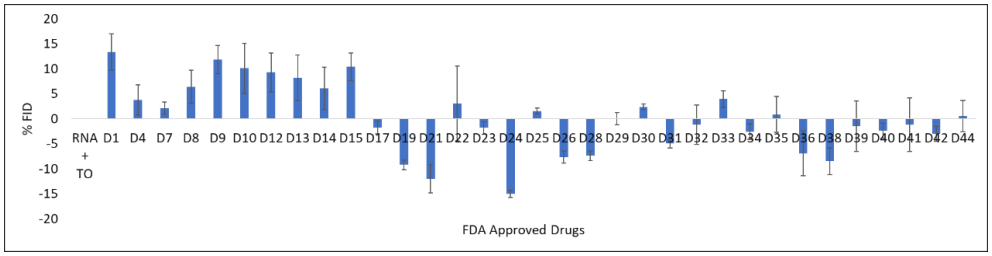

Figure 8 Percentage FID data of 5'CCG/3'CUG

For 5’CCG/3’CUG 16 drugs showed a reduction in the fluorescence value out of which D1 showed a maximum decrease in the fluorescence. The rest of the drugs showed an increase in fluorescence which is indicated in the graph.

3.3.5 FID – RNA 5’CAG/3’CCG – TO against 33 compounds

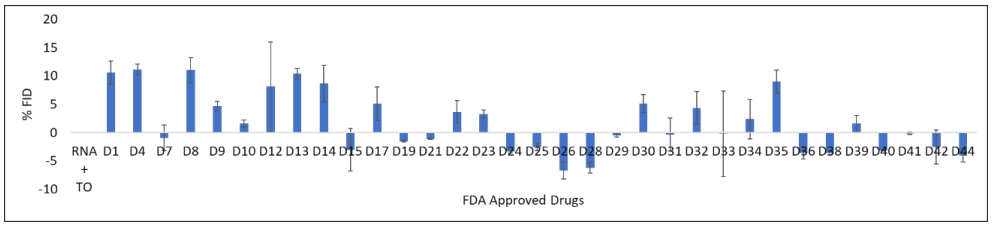

Figure 9 Percentage FID data of 5'CAG/3'CCG

For RNA having A-C mismatch i.e. 5’CAG/3’CCG many of the drugs showed a decrease in the fluorescence value as shown in the graph.

3.3.6 FID – RNA 5’CUG/3’CCG – TO against 33 compounds

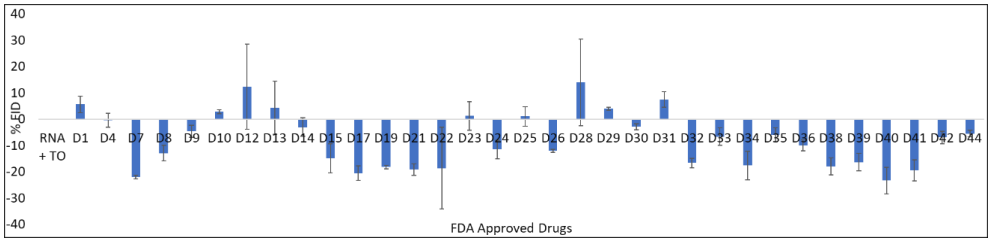

Figure 10 Percentage FID data of 5'CUG/3'CCG

For RNA 5’CUG/3’CCG seven drugs showed positive displacement values in which D28 showed maximum displacement.

3.3.7 FID – RNA 5’CAG/3’CAG – TO against 33 compounds

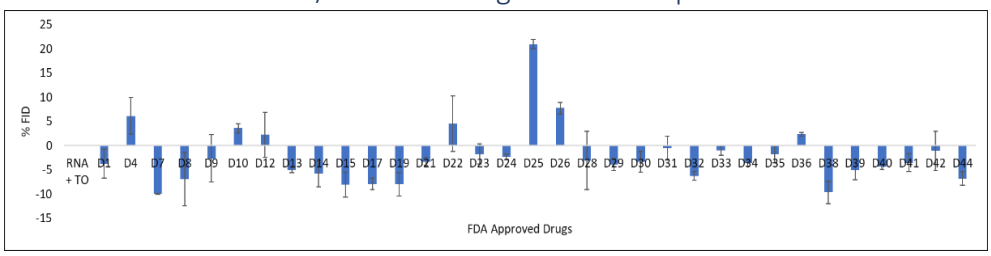

Figure 11 Percentage FID data of 5'CAG/3'CAG

In the case of 5’CAG/3’CAG which has A-A mismatch, 7 drugs showed a decrease in the fluorescence value out of which D25 showed maximum displacement of thiazole orange.

3.3.8 FID – RNA 5’CCG/3’CCG – TO against 33 compounds

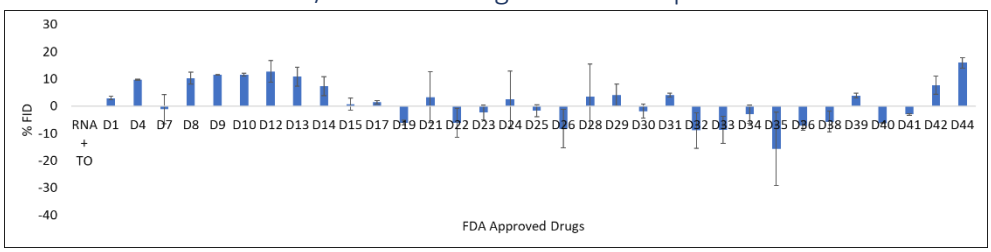

Figure 12 Percentage FID data of 5'CCG/3'CCG

For RNA 5’CCG/3’CCG having C-C mismatch more than 10 drugs showed positive displacement value out of these drugs D44 showed maximum displacement of thiazole orange.

3.3.9 FID – RNA 5’CUG/3’CUG – TO against 33 compounds

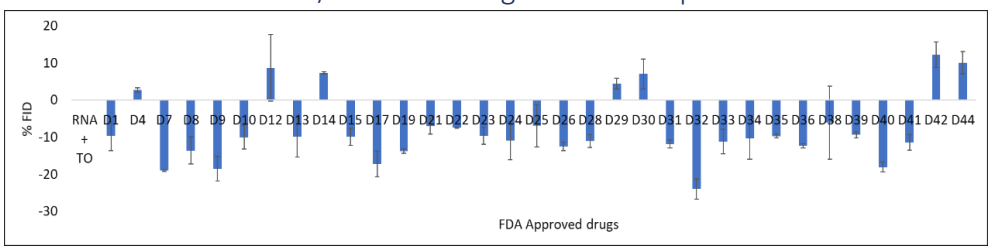

Figure 13 Percentage FID data of 5'CUG/3'CUG

For RNA having U-U mismatch i.e. 5’CUG/3’CUG, the D42 drug showed maximum reduction in the fluorescence value. Apart from these six other drugs as shown in the graph also showed a reduction in the fluorescence value.

3.3.10 FID – RNA 5’CAG/3’CUG – TO against 33 compounds

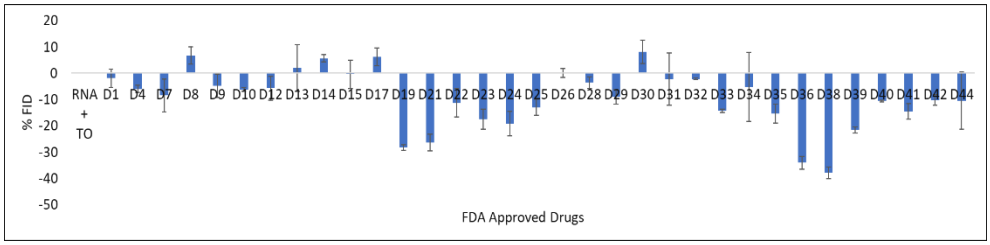

Figure 14 Percentage FID data of 5'CAG/3'CUG

5’CAG/3’CUG is control RNA i.e. it does not have any mismatch in this RNA A-U canonical matching takes place. Drugs that will show a decrease in the fluorescence value for this RNA will not be considered for further binding studies.

3.3.11 FID – RNA 5’CGG/3’CGG – TO against 33 compounds

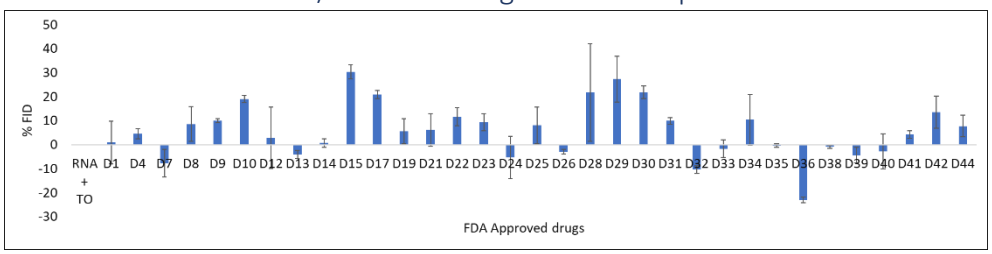

Figure 15 Percentage FID data of 5'CGG/3'CGG

5’CGG/3’CGG is the target RNA which has G-G mismatch. For this RNA various drugs showed positive displacement values. After comparing the displacement values with control RNA which is 5’CAG/3’CUG drugs D10, D15, D28 and D29 were selected as lead molecules as they showed maximum displacement for target while having no displacement value in the control RNA.

3.4 Fluorescence Binding Assay with Lead molecules

Fluorescence binding was performed with lead molecules having various internal 1*1 nucleotide mismatches like A-A, C-C, G-G and U-U. Along with these the binding assay was also performed with control RNA i.e. RNA having canonical A-U base pairing. Apart from these, binding assay was also performed with various CGG repeat like 20, 40 and 60.

3.4.1 Fluorescence Binding Assay D10 + RNA

Given below are fluorescence titration curves of RNA having various internal 1*1 loops with D10 compound. The K_D values are mentioned on bottom right side of the plot.

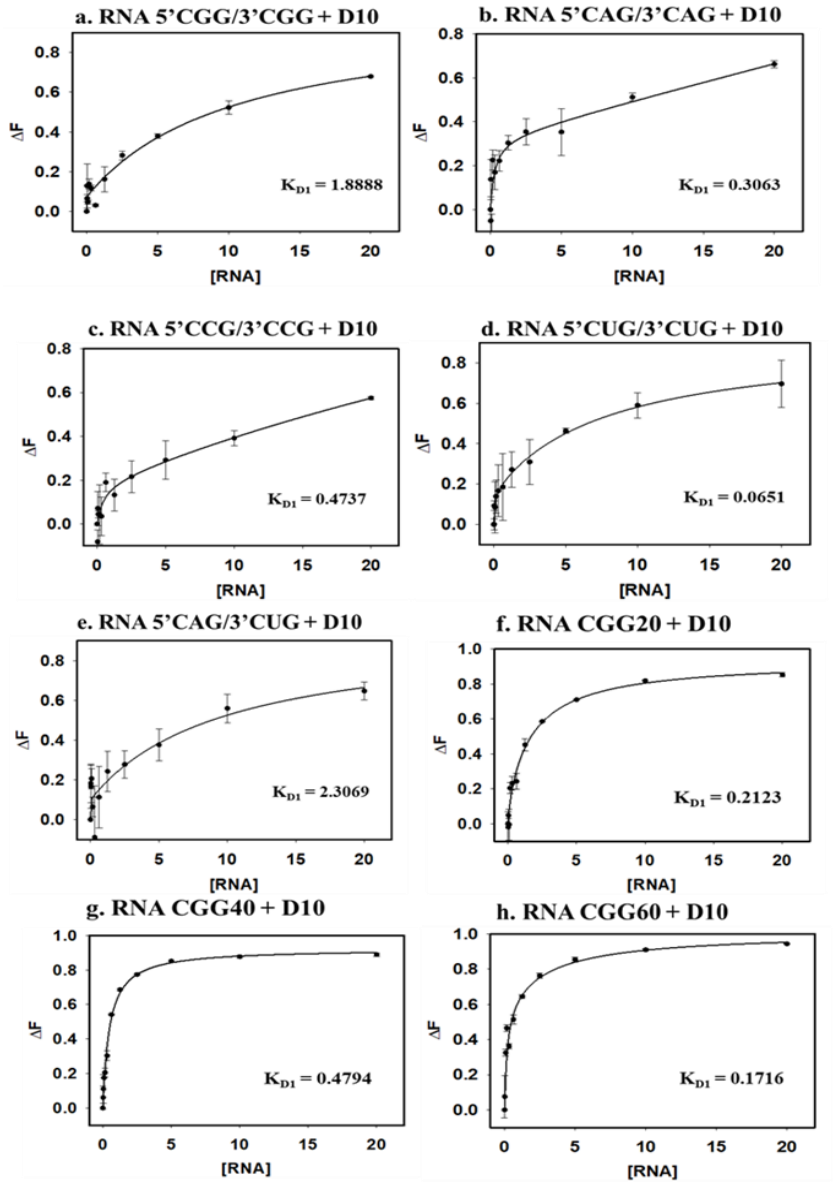

Figure 16 Fluorescence titration curves of various RNA with D10

Figure 16 illustrates fluorescence titration curves of various RNA with lead molecule D10. The below bar graph (Figure 17) represents K_D values of all of various RNA obtained after plotting the data with help of Sigma Plot software.

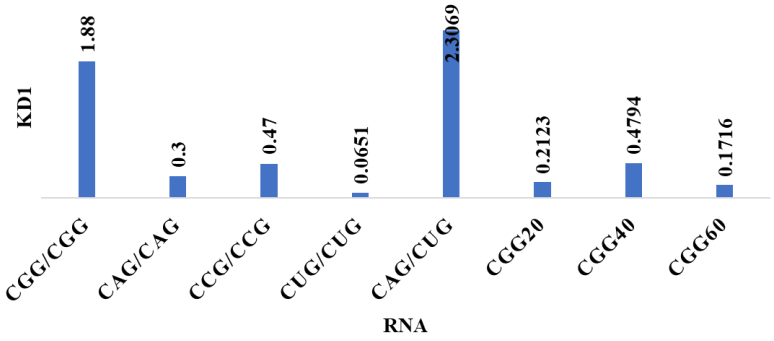

Figure 17 Bar graph representing K_D values

After performing fluorescence binding assay with help of sigma plot software K_D values were calculated which are represented in the above bar graph. Maximum K_D value was observed for control RNA. While the minimum K_D value was obtained for RNA 5'CUG/3'CUG.

3.4.2 Fluorescence Binding Assay D15 + RNA

Given below are fluorescence titration curves of RNA having various internal 1*1 loops with D15 compound. The K_D values are mentioned on bottom right side of the plot.

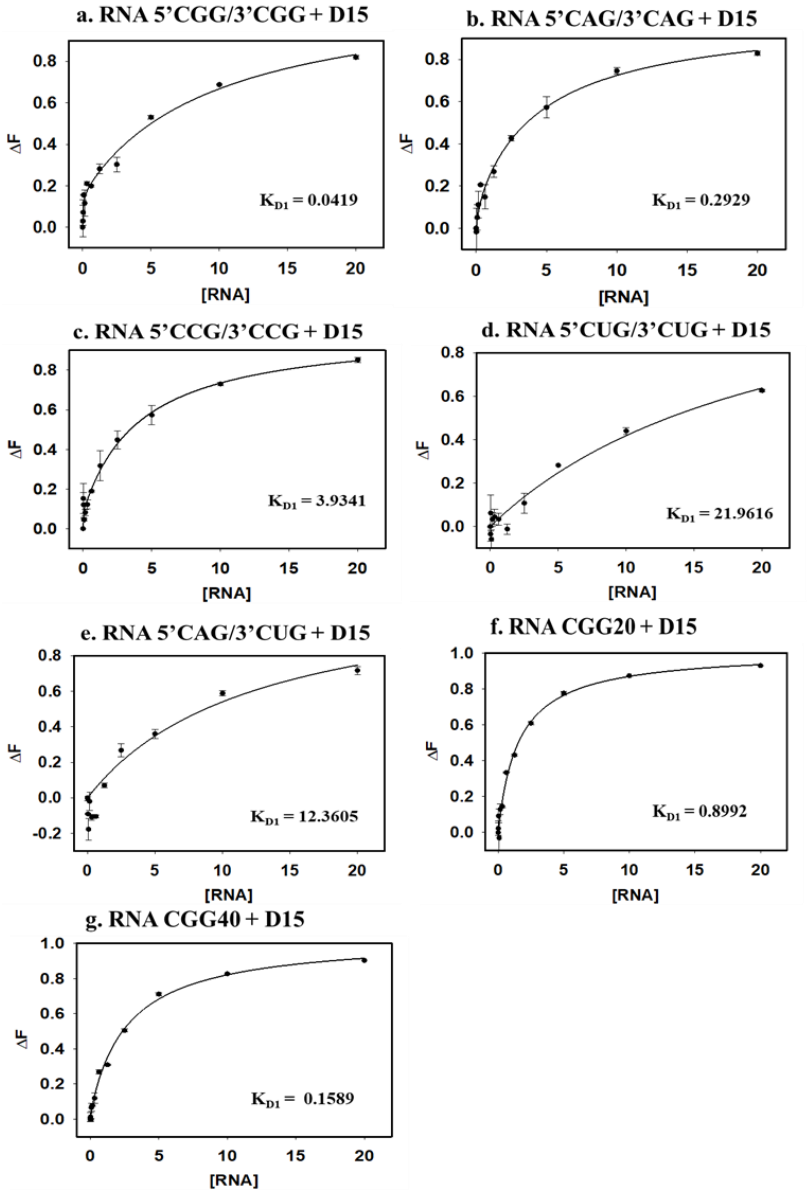

Figure 18 Fluorescence titration curves of various RNA with D15

Figure 18 illustrates fluorescence titration curves of various RNA with lead molecule D15. The below bar graph (Figure 19) represents K_D values of all of various RNA obtained after plotting the data with help of Sigma Plot software.

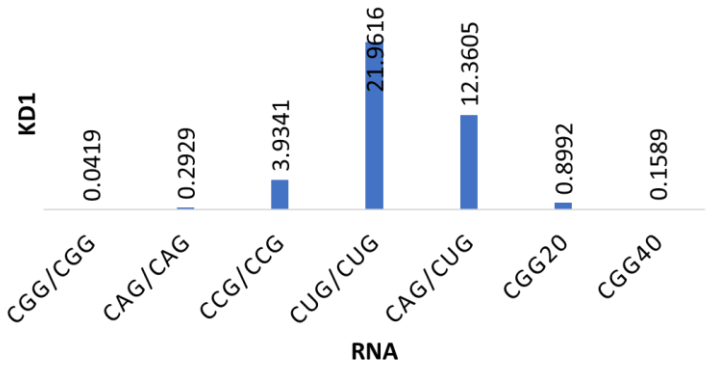

Figure 19 Bar graph representing KD values

As shown in the bar graph K_D value for 5'CGG/3'CGG was 0.0419 while K_D value for CGG20 and CGG40 were 0.8992 and 0.1589 respectively.

3.4.3 Fluorescence Binding Assay D25 + RNA

Given below are fluorescence titration curves of RNA having various internal 1*1 loops with D25 compound. The K_D values are mentioned on bottom right side of the plot.

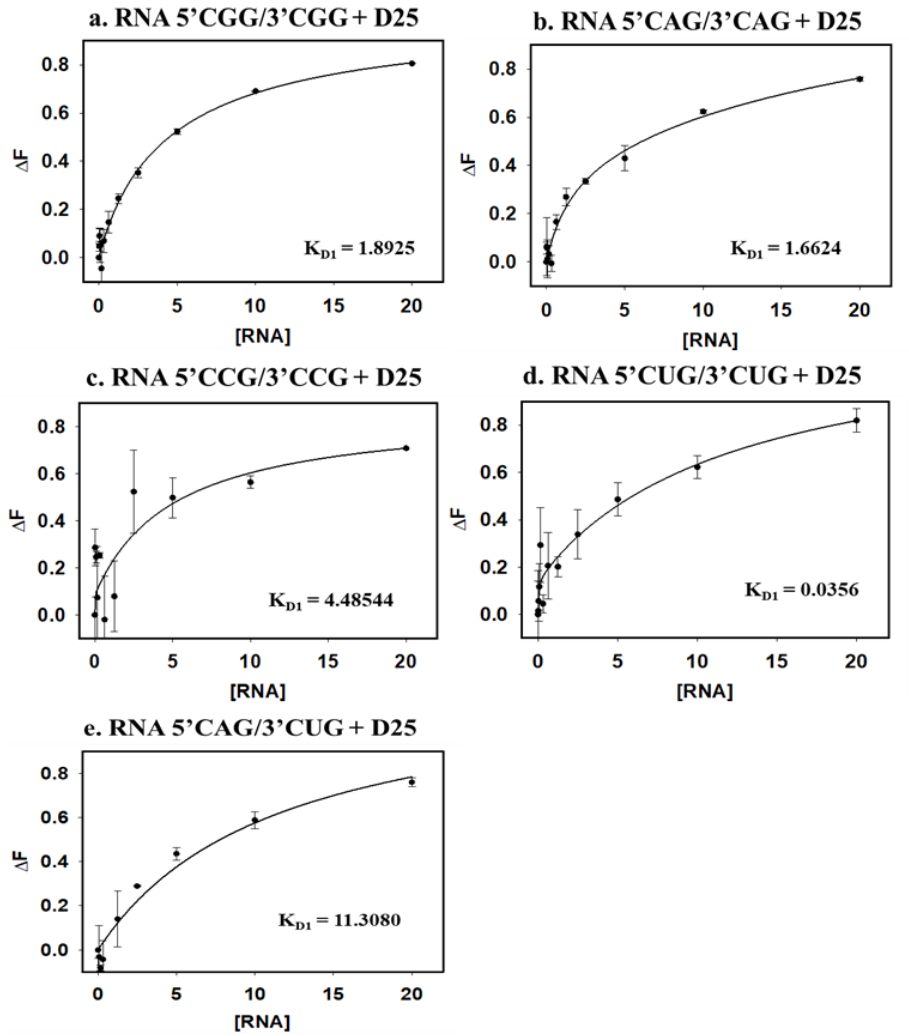

Figure 20 Fluorescence titration curves of various RNA with D25

Figure 20 illustrates fluorescence titration curves of various RNA with lead molecule D25. The below bar graph (Figure 21) represents K_D values of all of various RNA obtained after plotting the data with help of Sigma Plot software.

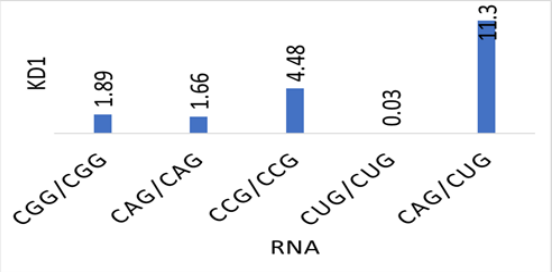

Figure 21 Bar graph representing KD values

Lowest K_D value was observed for RNA 5'CUG/3'CUG while for control RNA it was 11.3.

3.4.4 Fluorescence Binding Assay D29 + RNA

Given below are fluorescence titration curves of RNA having various internal 1*1 loops with D29 compound. The KD values are mentioned on bottom right side of the plot.

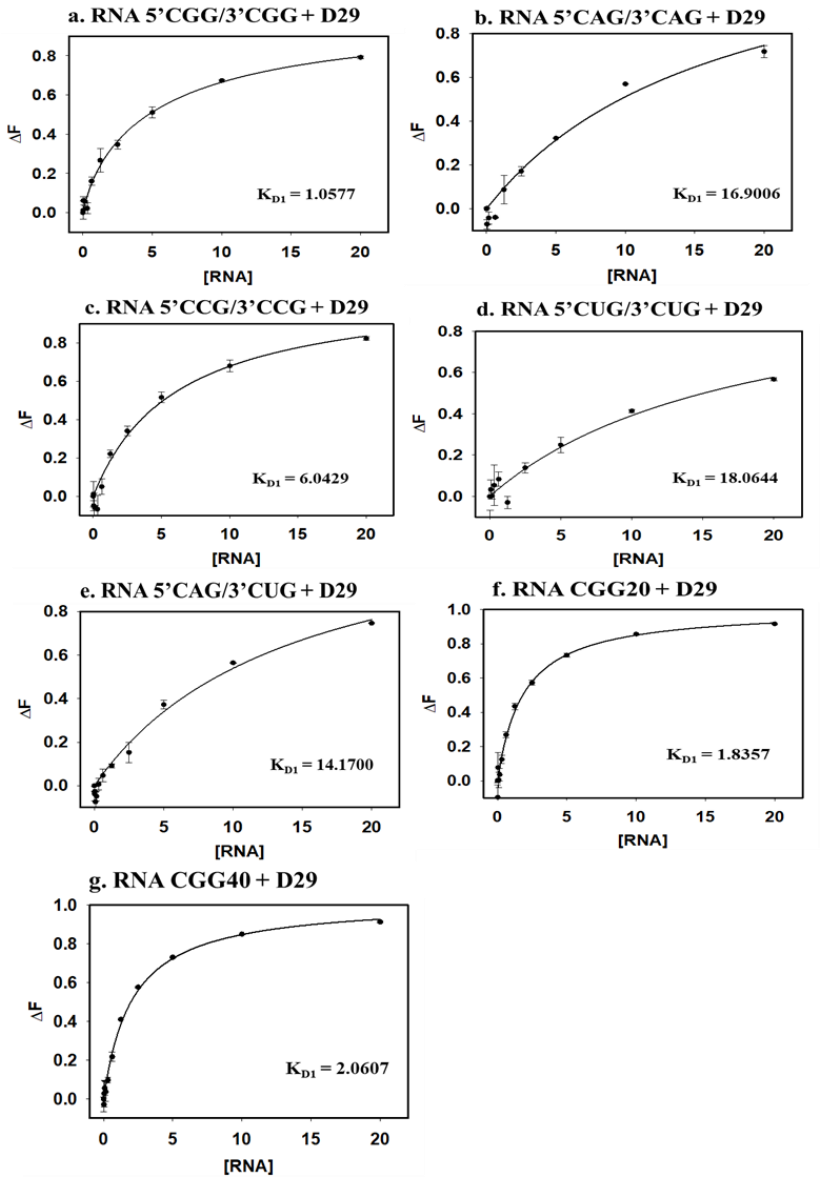

Figure 22 Fluorescence titration curves of various RNA with D29

Figure 22 illustrates fluorescence titration curves of various RNA with lead molecule D29. The below bar graph (Figure 23) represents K_D values of all of various RNA obtained after plotting the data with help of Sigma Plot software.

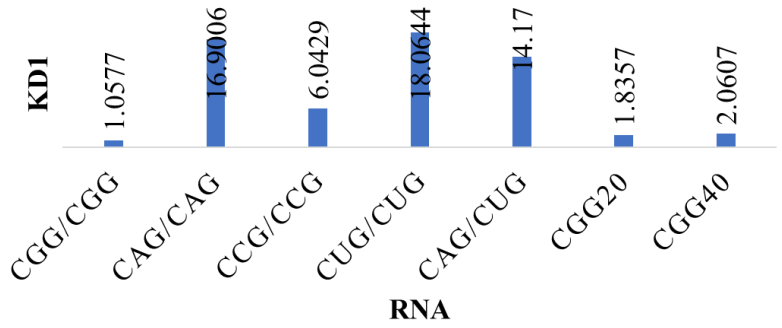

Figure 23 Bar graph representing KD values

K_D value for control was 14.17 while the same for target RNA 5'CGG/3'CGG was 1.0577. While for CGG20 and CGG40 repeat RNA it was 1.8357 and 2.0607 respectively.

3.5 Isothermal titration calorimetry (ITC) assay

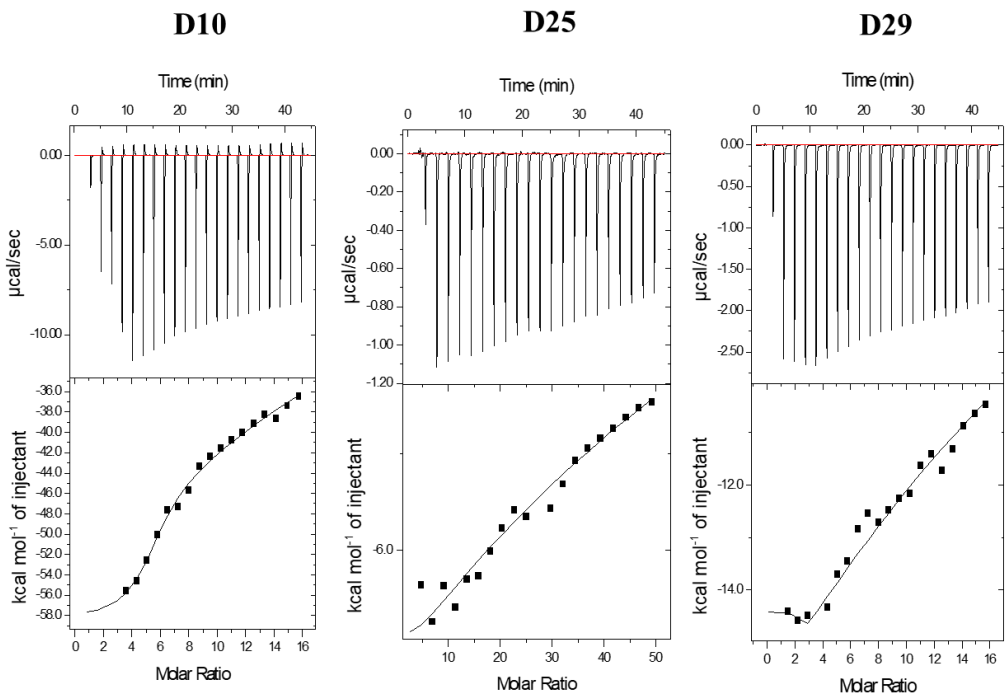

Figure 24 Isothermal titration calorimetric assay

Figure 24 shows Isothermal titration calorimetric assay measuring the energetics of RNA and compounds interactions. The top panel shows the power versus time curve while bottom panel shows the thermogram of the integrated peak intensities plotted against molar ratio. These represent curves of compound D10, D25 and D29 with RNA 5'CGG/3'CGG.

The K_D values for D10, D25 and D29 were 0.239 µM, 0.925 µM and 1.62 µM respectively.

3.6 Effects of FDA Drug on protein aggregation and accumulation in FXTAS Cell Model

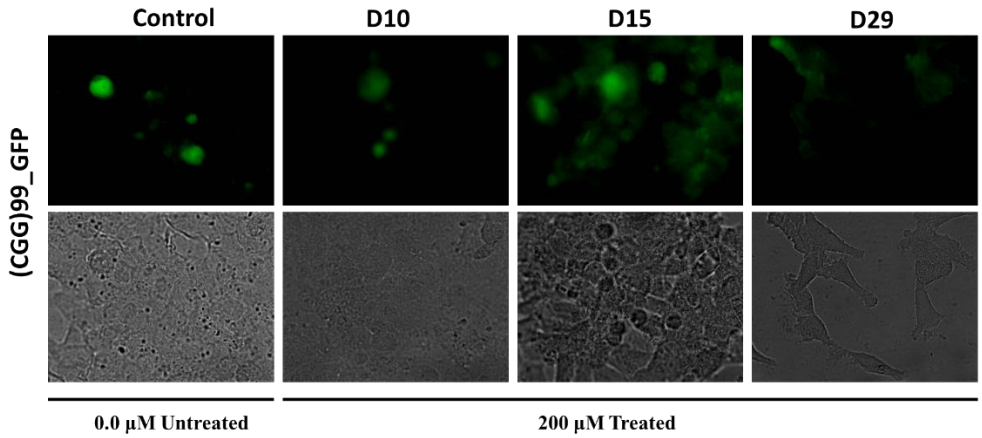

Figure 25 Effects of FDA Drug on protein aggregation and accumulation in FXTAS Cell Model

The above figure shows effect of drug treatment of protein aggregation and accumulation in FXTAS cell model. In control no drug was added. As we can see in the figure after drug treatment decrease in protein aggregation is seen. The most prominent decrease in the aggregation and accumulation is seen in D29.

Chapter 4 : Conclusions and Future prospects

For Fragile X-associated tremor/ataxia syndrome there is strong need of effective and safe medications. Recent studies in this field have reported that small molecules stabilize the CGG repeat RNA and thus ameliorates pathogenic defects associated with FXTAS[46]. In this study we have screened FDA-approved small molecules for their binding potential with CGG repeat RNA. After screening we found lead molecules which selectively bind to the CGG repeat RNA. These lead molecules were then further studied for their binding potential with the CGG repeat RNA. For further studying the binding potential of these lead molecules we performed fluorescence binding assay. Cell based assay of these molecules was also performed in which the effect of these molecules on protein aggregates of FXTAS cell model was observed. Significant decrease in protein aggregates was seen in case of D29 lead molecule. This suggests that D29 is able to prevent the non-canonical translation of CGG repeat RNA which causes toxic FMRPolyG protein. Along with D29 other lead molecules D10, D15 also showed decrease in the protein aggregation. These lead molecules are FDA-approved thus they can be used as therapeutic agents for treatment of FXTAS. Further studies have to be done to check whether these lead molecules are able to improve the splicing defect caused by the expression of CGG expansion. Further animal model studies are required to confirm whether these lead molecules can be used as therapeutic agents for the treatment of FXTAS.

Chapter 5 : References

1. Fu, Y. H. *et al.* Variation of the CGG repeat at the fragile X site results in genetic instability: resolution of the Sherman paradox. *Cell* **67**, 1047–1058 (1991).
2. Spada, A. R. L., Wilson, E. M., Lubahn, D. B., Harding, A. E. & Fischbeck, K. H. Androgen receptor gene mutations in X-linked spinal and bulbar muscular atrophy. *Nature* **352**, 77–79 (1991).
3. López Castel, A., Cleary, J. D. & Pearson, C. E. Repeat instability as the basis for human diseases and as a potential target for therapy. *Nat. Rev. Mol. Cell Biol.* **11**, 165–170 (2010).
4. Krzyzosiak, W. J. *et al.* Triplet repeat RNA structure and its role as pathogenic agent and therapeutic target. *Nucleic Acids Res.* **40**, 11–26 (2012).
5. Verma, A. K., Khan, E., Bhagwat, S. R. & Kumar, A. Exploring the Potential of Small Molecule-Based Therapeutic Approaches for Targeting Trinucleotide Repeat Disorders. *Mol. Neurobiol.* **57**, 566–584 (2020).
6. Verma, A. K. *et al.* Curcumin Regulates the r(CGG)exp RNA Hairpin Structure and Ameliorate Defects in Fragile X-Associated Tremor Ataxia Syndrome. *Front. Neurosci.* **14**, (2020).
7. Lozano, R., Azarang, A., Wilaisakditipakorn, T. & Hagerman, R. J. Fragile X syndrome: A review of clinical management. *Intractable Rare Dis. Res.* **5**, 145–157 (2016).
8. Ciaccio, C. *et al.* Fragile X syndrome: a review of clinical and molecular diagnoses. *Ital. J. Pediatr.* **43**, 39 (2017).
9. Martin, J. P. & Bell, J. A PEDIGREE OF MENTAL DEFECT SHOWING SEX-LINKAGE. *J. Neurol. Psychiatry* **6**, 154–157 (1943).
10. A marker X chromosome. - PMC.
11. Rueda, J.-R., Ballesteros, J., Guillen, V., Tejada, M.-I. & Solà, I. Folic acid for fragile X syndrome. *Cochrane Database Syst. Rev.* (2011) doi:10.1002/14651858.CD008476.pub2.
12. Hall, S. S. Treatments for fragile X syndrome: A closer look at the data. *Dev. Disabil. Res. Rev.* **15**, 353–360 (2009).
13. Wirojanan, J. *et al.* The efficacy of melatonin for sleep problems in children with autism, fragile X syndrome, or autism and fragile X

syndrome. *J. Clin. Sleep Med. JCSM Off. Publ. Am. Acad. Sleep Med.* **5**, 145–150 (2009).

14. Advances in the Treatment of Fragile X Syndrome | Pediatrics | American Academy of Pediatrics.
15. Turk, J. Fragile X syndrome: lifespan developmental implications for those without as well as with intellectual disability. *Curr. Opin. Psychiatry* **24**, 387–397 (2011).
16. Moskowitz, L. J., Carr, E. G. & Durand, V. M. Behavioral Intervention for Problem Behavior in Children With Fragile X Syndrome. *Am. J. Intellect. Dev. Disabil.* **116**, 457–478 (2011).
17. Hessl, D. *et al.* The influence of environmental and genetic factors on behavior problems and autistic symptoms in boys and girls with fragile X syndrome. *Pediatrics* **108**, E88 (2001).
18. Hagerman, R. J. *et al.* Intention tremor, parkinsonism, and generalized brain atrophy in male carriers of fragile X. *Neurology* **57**, 127–130 (2001).
19. Tassone, F. *et al.* Elevated Levels of FMR1 mRNA in Carrier Males: A New Mechanism of Involvement in the Fragile-X Syndrome. *Am. J. Hum. Genet.* **66**, 6–15 (2000).
20. Tassone, F. *et al.* Intranuclear inclusions in neural cells with premutation alleles in fragile X associated tremor/ataxia syndrome. *J. Med. Genet.* **41**, e43 (2004).
21. Van Esch, H. *et al.* Screening for FMR-1 premutations in 122 older Flemish males presenting with ataxia. *Eur. J. Hum. Genet.* **13**, 121–123 (2005).
22. Brussino, A. *et al.* FMR1 gene premutation is a frequent genetic cause of late-onset sporadic cerebellar ataxia. *Neurology* **64**, 145–147 (2005).
23. Dombrowski, C. *et al.* Premutation and intermediate-size FMR1 alleles in 10572 males from the general population: loss of an AGG interruption is a late event in the generation of fragile X syndrome alleles. *Hum. Mol. Genet.* **11**, 371–378 (2002).
24. Rousseau, F., Rouillard, P., Morel, M. L., Khandjian, E. W. & Morgan, K. Prevalence of carriers of premutation-size alleles of the FMRI gene--and implications for the population genetics of the fragile X syndrome. *Am. J. Hum. Genet.* **57**, 1006–1018 (1995).

25. Jacquemont, S. *et al.* Penetrance of the Fragile X–Associated Tremor/Ataxia Syndrome in a Premutation Carrier Population. *JAMA* **291**, 460–469 (2004).
26. Jacquemont, S. *et al.* Fragile X Premutation Tremor/Ataxia Syndrome: Molecular, Clinical, and Neuroimaging Correlates. *Am. J. Hum. Genet.* **72**, 869–878 (2003).
27. Botez, M. I. *et al.* Amantadine hydrochloride treatment in heredodegenerative ataxias: a double blind study. *J. Neurol. Neurosurg. Psychiatry* **61**, 259–264 (1996).
28. Zesiewicz, T. A. & Sullivan, K. L. Treatment of Ataxia and Imbalance With Varenicline (Chantix): Report of 2 Patients With Spinocerebellar Ataxia (Types 3 and 14). *Clin. Neuropharmacol.* **31**, 363–365 (2008).
29. Impaired Endothelial Function in Young Women with Premature Ovarian Failure: Normalization with Hormone Therapy | The Journal of Clinical Endocrinology & Metabolism | Oxford Academic.
30. Effect of early menopause on bone mineral density and fractu... : Menopause.
31. Atsma, F., Bartelink, M.-L. E. L., Grobbee, D. E. & van der Schouw, Y. T. Postmenopausal status and early menopause as independent risk factors for cardiovascular disease: a meta-analysis. *Menopause* **13**, 265–279 (2006).
32. Disney, M. D. *et al.* A Small Molecule that Targets r(CGG)exp and Improves Defects in Fragile X-Associated Tremor Ataxia Syndrome. *ACS Chem. Biol.* **7**, 1711–1718 (2012).
33. Qurashi, A. *et al.* Chemical screen reveals small molecules suppressing fragile X premutation rCGG repeat-mediated neurodegeneration in Drosophila. *Hum. Mol. Genet.* **21**, 2068–2075 (2012).
34. Kumari, D. & Usdin, K. Sustained expression of FMR1 mRNA from reactivated fragile X syndrome alleles after treatment with small molecules that prevent trimethylation of H3K27. *Hum. Mol. Genet.* **25**, 3689–3698 (2016).
35. Zhu, X. *et al.* Synthesis and characterization of a bifunctional nanoprobe for CGG trinucleotide repeat detection. *RSC Adv.* **7**, 36124–36131 (2017).

36. Verma, A. K., Khan, E., Mishra, S. K., Jain, N. & Kumar, A. Piperine Modulates Protein Mediated Toxicity in Fragile X-Associated Tremor/Ataxia Syndrome through Interacting Expanded CGG Repeat (r(CGG)exp) RNA. *ACS Chem. Neurosci.* **10**, 3778–3788 (2019).

37. Milligan, J. F. & Uhlenbeck, O. C. [5] Synthesis of small RNAs using T7 RNA polymerase. in *Methods in Enzymology* vol. 180 51–62 (Academic Press, 1989).

38. Wolf, D. E. Fundamentals of fluorescence and fluorescence microscopy. *Methods Cell Biol.* **114**, 69–97 (2013).

39. Shivalingam, A. *et al.* The interactions between a small molecule and G-quadruplexes are visualized by fluorescence lifetime imaging microscopy. Nat. Commun. **6**, 8178 (2015).

40. Velazquez-Campoy, A. & Freire, E. Isothermal titration calorimetry to determine association constants for high-affinity ligands. *Nat. Protoc.* **1**, 186–191 (2006).

41. Duff, M. R., Grubbs, J. & Howell, E. E. Isothermal titration calorimetry for measuring macromolecule-ligand affinity. *J. Vis. Exp. JoVE* 2796 (2011) doi:10.3791/2796.

42. Freyer, M. W. & Lewis, E. A. Isothermal titration calorimetry: experimental design, data analysis, and probing macromolecule/ligand binding and kinetic interactions. *Methods Cell Biol.* **84**, 79–113 (2008).

43. Holden, N. S. & Tacon, C. E. Principles and problems of the electrophoretic mobility shift assay. *J. Pharmacol. Toxicol. Methods* **63**, 7–14 (2011).

44. Hellman, L. M. & Fried, M. G. Electrophoretic Mobility Shift Assay (EMSA) for Detecting Protein-Nucleic Acid Interactions. *Nat. Protoc.* **2**, 1849–1861 (2007).

45. Fillebeen, C., Wilkinson, N. & Pantopoulos, K. Electrophoretic mobility shift assay (EMSA) for the study of RNA-protein interactions: the IRE/IRP example. *J. Vis. Exp. JoVE* (2014) doi:10.3791/52230.

46. Yang, W.-Y. *et al.* Small Molecule Recognition and Tools to Study Modulation of r(CGG)(exp) in Fragile X-Associated Tremor Ataxia Syndrome. *ACS Chem. Biol.* **11**, 2456–2465 (2016).